arXiv:1401.3098v2 [cs.IT] 16 Mar 2014

Interference Alignment (IA) and Coordinated Multi-Point (CoMP) overheads and RF impairments: testbed results

Per Zetterberg
Access Linnaeus Center
KTH Royal Institute of Technology, Osquldas väg 10,
SE-100 44 Stockholm, Sweden,
Email: perz@ee.kth.se

***Abstract*—In this work we investigate the network MIMO techniques of interference alignment (IA) and joint transmission coordinated multipoint (CoMP) in an indoor very small cell environment. Our focus is on the overheads in a system with quantized channel state feedback from the receiver to the transmitter (based on the 802.11ac standard) and on the impact of non-ideal hardware. The indoor office scenario should be the most favorable case in terms of the required feedback rates due to the large coherence bandwidth and coherence time of the channel. The evaluations are done using a real-world wireless testbed with three BSs and three MSs all having two antennas. The signal to noise ratio in the measurements is very high, 35-60dB, due to the short transmission range. Under such conditions radio hardware impairments becomes a major limitation on the performance. We quantify the impact of these impairments. For a 23ms update interval the overhead is 2.5% and IA and CoMP improves the sum throughput 27% and 47% in average (over the reference schemes e.g. TDMA MIMO), under stationary conditions. When two people are walking in the measurement area the throughput improvements drops to 16% and 45%, respectively.**

I. Introduction

Network MIMO techniques has been the focus of much research interest, see e.g. [1]. An overview of some 3GPP work and results in the area can be found in [2]. The feedback schemes standardized in 3GPP are focused on reporting channel quality information (CQI) and precoder matrix index (PMI) of a few transmission and interference hypotheses rather than providing full channel state information (channel matrices) to the transmitters, [2]. In much of the more academic work in the area, full channel state information CSI is a common assumption. Such full information incurs a high overhead that may be hard to justify in outdoor scenarios with significant mobility. In this work we focus on an indoor very dense scenario where full CSI may still be a worthwhile option to pursue. The latest WiFi standard 802.11ac, aimed at such environments incorporates a feedback scheme which provides the transmitter with almost full channel state information for the MU-MIMO scenario (single access point serving multiple users). Herein we use the feedback compression scheme of that standard in a network MIMO context in the form of coordinated multipoint (CoMP) and interference alignment (IA). Although we use a feedback scheme from the WiFi domain, a similar scheme could be introduced also in cellular systems aimed at the same environment.

A breakthrough in information theory was achieved with "interference alignment" which was presented in the paper [3]. According to the theory, $K/2$, interference free modulation streams can be created in a system with K links (K transmitters and K receivers), even with only a single antenna at each node. The catch is, to achieve this capacity; linear precoding over multiple channel realizations (channel extensions) is needed besides global channel knowledge. The most practical implementation of channel extensions is probably to utilize the subcarriers of an OFDM modulation thereby creating diagonal MIMO channels. However the required number of subcarriers grows extremely fast with K. Results under more realistic assumptions have so far been modest [4].

Interference alignment (IA) can also be applied without channel extensions using multiple antennas (i.e. on MIMO channels) in a way that is in fact a version of coordinated beamforming, see e.g. [5], [6]. The interference alignment theory in [3], provides us with a closed solution to the problem of creating $KM/2$ interference free modulation streams in a system with $K = 3$ links where each node has M antennas.

In this paper we study the scenario with three BSs and three MSs with two antennas each. We use the MIMO version of interference alignment as described above. In addition we also investigate a form of coordinated multipoint transmission where all six transmitter antennas in the system are used collectively as a single coherent antenna array to optimize the signal to interference ratio of all users.

This paper includes not only simulation results but also measurements. Moreover, we do not just perform simulations based on channel measurements but present over-the-air actual transmissions over the channel. By doing so we establish a "ground truth" of what is achievable with IA and CoMP. Note that the true wireless channel from the base-band of

This work was done within the framework of the Swedish SSF sponsored RAMCOORAN project and the EU project RAMCOORAN. The HiATUS project acknowledges the financial support of the Future and Emerging Technologies program within FP7 for Research of the European Commission (FET Open grant number 265578).

the transmitter to the base-band of the receiver does not only involve the radio propagation channel but also the impact of the analog hardware of the transmitter and receiver. This effect includes e.g. the impact of amplifier non-linearities and phase-noise, [7]. In this paper we use transmitters and receivers with error vector magnitudes (EVM) of 1-4%, see Section 4, which is reasonable model of consumer-grade wireless equipment.

Previous work on experimentation within IA and CoMP includes the papers [8]–[15]. A short summary of some of the main findings in these papers are given in Section I of [12]. In this paper, as in [12], we use the feedback compression scheme defined for MU-MIMO in the IEEE802.11ac standard but applied to IA and COMP, in an indoor office environment. *This paper has the following novel aspects*, 1) the impact of people walking in the measurement environment (time varying channels) is studied experimentally, 2) the overhead of perfoming IEEE802.11ac feedback is studied in IA and CoMP scenarios, 3) we factor out the impact of hardware impairments (the methodology as well as the results) , 4) we use an impairment model based on look-up tables of error vector magnitude (EVM) versus RMS signal strength and investigate its applicability,

The feedback update rate is 23ms and we investigate the performance at the end of this update period. By using a combination of measurements and simulations we also analyze a 3ms update interval, in Section V-C. For our system the overhead, using the IEEE802.11ac standard, is 2.5%; see Section III-B. IA and CoMP improves the sum throughput 27% and 47% in average (over the reference schemes e.g. TDMA MIMO), under stationary conditions. When two people are walking in the measurement area the throughput improvements drops to 16% and 42%, respectively. Unfortunately, due to implementation difficulties related to computational loads and system latencies in our PC based implementation, we are not able to reduce the update interval. However, by using a combination of simulation and measurements we estimate that IA can improve its sum throughput from 11.0bits/sec/subcarrier to 11.6bits/sec/subcarrier by using a 3ms update interval, see Section V-C.

The *general conclusions* from the present paper is that IA and CoMP can provide an improvement over the reference schemes even when considering a realistic feedback scheme and channel variations albeit in one of the most favorouble scenarios. At the same time, the paper also shows that the performance is lower than what would be predicted by simulations based on channel measurements in the same environment. This highlights the necesity of considering hardware impairments in system analysis. We also use a commonly employed hardware impairment model. In order to get a good match between simulation and measurements, we have made look-up tables of EVM versus signal strength. Despite this effort, there is still a discrepancy between measurement and simulation results. This result motivates further research into the issue and the use of over-the-air performance evaluations to obtain truly realistic results. The results also show that CoMP is less sensitive than IA to channel variations and hardware impairments, where both schemes use the same number of spatial streams.

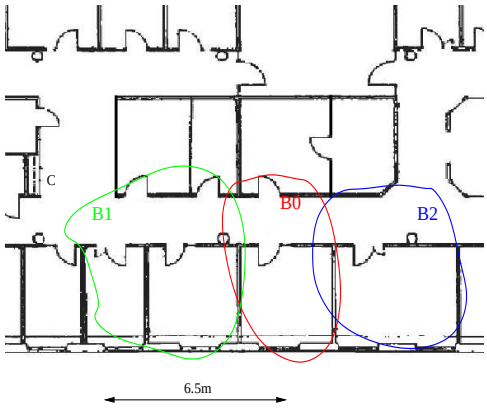

Fig. 1. Map over the measurement area

The paper is organized as follows. In Section II we give an overview of the testbed. Section III describes the signal processing including the MS to BS feedback mechanisms. The hardware impairment model is described in Section 4. The measurement results are provided in Section V. Finally, our conclusions are summarized in Section VI.

II. Hardware Overview

We consider a scenario with three links. The propagation environment is indoor office. A map of the measurement area is shown in Figure 1. The positions of the three base-stations are marked “B0”, “B1” and “B2”. The red, green and blue area shows the coverage area of each BS (i.e. the corresponding MS was moved around in this area during the measurements, each one of the three BSs easily covers all the areas in terms of SNR). A picture taken from the location marked “C” in the map is shown in Figure 2. In the picture, the base-station antennas of BS A are visible as well as some of the testbed hardware.

The BSs consists of two USRP N210 with XCVR2450 daughterboards (see www.ettus.com). They are connected to mini-circuits (see www.minicircuits.com) ZRL-2400LN amplifiers which in turn are connected to two vertically polarized antennas which are hanging down from the ceiling. The base-band signals are generated by a PC which are connected to the USRPs using ten meter Gigabit Ethernet cables.

The MSs also uses two USRP N210. Here we are however using custom made RF front-ends; see [16]. The base-band signal is then sampled by the USRP N210s. The system operates at 2490MHz. The receivers are also connected to a PC using ten meter Gigabit Ethernet cables.

The processing of all three BSs runs on the same PC as separate threads. Likewise all the three MSs runs on another PC, as separate threads. The MS to BS feedback is done over wired Ethernet, but compressed according to Section III-B. All the software is available as open source at sourceforge.net under the project names `fourmulti` and `iacomp`.

The thermal noise standard deviation is roughly the same, $\sigma^2_{\text{nominal}}$, in all receivers. This value is known by all nodes.

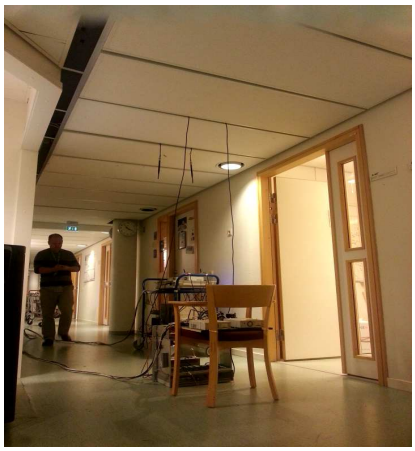

Fig. 2. Picture of measurement setup

III. Implementation

A. Air Interface and Signal Processing Overview

We use an OFDM modulation scheme with a subcarrier spacing of 312.5kHz, coinciding with that of 802.11a/n/ac. The cyclic prefix is 0.4μs and thus the symbol time 3.6μs. Due to limited sampling speeds of the USRP only 38 subcarriers are used instead of the (at least) 58 used by 802.11n/ac. Two pilot subcarriers are inserted in each symbol at +7 and -7th subcarriers from the center frequency, and used for common phase error correction.

Ten different coding and modulation schemes (MCSs) have been implemented ranging from one to six bit/symbol/subcarrier using QPSK to 256QAM constellations and LDPC codes of rate 1/2 to 3/4.

In each run of the system, two frames are transmitted. The first frame contains only six known training symbols transmitted sequentially from the six BS antennas in the system. This frame takes the function of the null data packet (NDP) in MU-MIMO feedback of the IEEE802.11ac standard, see [17].

The MSs estimate the 2×6 matrix channel from all six base-station antennas to its two antennas. The MSs then compress the channel estimatesw, according to the IEEE802.11ac standard (as described in Section III-B) and sends the result to the BS which unpacks it.

The BSs then calculates the beamformers as described in Section III-C, and sends a second frame using these. This frame is sent simultaneously from all the three BSs 20ms after the first frame. The frame is 3.2ms and consists of six identical subframes (in order to provide statistics for our evaluation). The spacing between the subframes is 0.5ms. Each subframe has two training blocks. Each training block is formatted as shown in Figure 3. First six symbols are transmitted sequentially from the six BS transmitter antennas (C0-C5). These symbols are not used by the receiver, but will turn out to be very useful in our analysis of the system. The following three symbols are training symbols corresponding to the three simultaneously transmitted streams (D0-D2). These

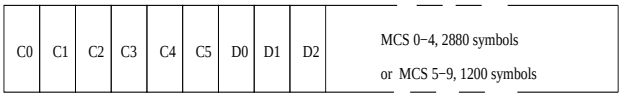

Fig. 3. Training block

symbols correspond to demodulation reference symbols in LTE nomenclature and correspond to the VHT-LTF field in 802.11ac. These symbols are used in the receiver to calculate the weights of a structured MMSE combiner. Last in the training block are the payload symbols (actually the vast majority of symbols). In the first training block, these symbols are encoded using MCS 0 to 4, corresponding to rates 1-2.5 bits/subcarrier/symbol. In the second training block, MCSs with rates of 3-6 bits/subcarrier/symbol are transmitted. The reason for dividing the subframes into two training blocks is to avoid the need for adaptive receiver algorithms.

In the evaluation of the system, we focus on the sum throughput. We measure the sum throughput by decoding the received bits and determine the highest MCS for which there are no bit errors i.e. when the frame is successfully decoded. By doing so a practically achievable rate is obtained. Due to the six subframes in the burst, six throughput measurements are obtained per frame.

In a commercial system, the latency of 20ms is unacceptable. However, a training repetition time of 23ms could be considered as an option with low overhead. In such as case, our measurements correspond to the performance at the end of the update period.

B. Feedback

The standardized feedback scheme of IEEE802.11ac is derived in [18] where it is called “simple feedback method for slowly time-varying channels”. In the scheme, the channel matrix is first decomposed using a singular value decomposition as

$$\mathbf{H} = \mathbf{USV}^H. \tag{1}$$

In our case, the matrix $\mathbf{H}$, is the channel between all six transmitter antennas in the system and the two antennas at the mobile station. According to the feedback scheme, the $\mathbf{V}$ matrix is encoded into two sets of angles, ϕ and ψ, using a procedure which is similar to QR decomposition using Givens rotations. The number of ϕ and ψ angles are both $mn-n/2-n^2/2$, where m is the number of BS antennas and n the number MS antennas. Using b_ϕ and b_ψ bits respectively to quantize the ϕ and ψ angles, the number of bits needed in total to encode one $\mathbf{V}$ matrix is $((2m-1)n-n^2)(b_\phi+b_\psi)/2$. The number of bits for the angles b_ϕ and b_ψ (see above), can have the values $b_\phi = 5$ and $b_\psi = 7$ or $b_\phi = 7$ and $b_\psi = 9$ according to the standard. Herein, only the latter value has been used. We refer to [18] and our previous paper [12] for more details on the procedure of obtaining the angles (see also our Matlab/Octave implementation at http://people.kth.se/~perz/packV/). The diagonal $\mathbf{S}$ matrix is also fed back. After dividing the diagonal elements of the

matrix with the standard deviation of the noise, the result corresponds to the square root of the SNR of the corresponding stream. These SNRs are quantized and sent to the transmitter together with the encoding of the $\mathbf{V}$ matrix.

Since we are using an OFDM modulation scheme, there is actually one channel matrix per subcarrier. Since adjacent subcarriers will experience similar channels, it is not necessary to feed back the channel matrix for every subcarrier. The IEEE802.11ac standard defined as parameter N_g. When $N_g = 4$, the channel is only reported on every fourth subcarrier. In this paper we will use $N_g = 8$ which is actually not defined in the standard but which turned out to be sufficient in our environment according to the measurements in [12].

Thus since $N_g = 8$ the ϕ and ψ values are reported for every eighth subcarrier which means four $\mathbf{V}$ matrices in our case. The SNRs are quantized in two steps. First an average SNR is calculated for all the reported subcarriers. This average is then uniformly quantized with eight bits in the range from -10dB to 53.75dB. The SNR is then reported with half of the granularity of the $\mathbf{V}$ matrix. The SNR on a certain subcarrier is then encoded as the difference between the average SNR and the SNR of that particular subcarrier (this is done for each streams individually). This value is quantized between -8dB and 7dB using four bits i.e. using a one dB granularity. The number of feedback bits required (per sub-carrier) is given by

$$n_{\text{feedback per subcarrier}} = ((2m-1)n - n^2)(b_\phi + b_\psi)/(2N_g) + 4/N_g + 16/N_c, \quad (2)$$

where N_c is the total number of subcarriers. In our case, $m = 6$, $n = 2$, $N_g = 8$, $N_c = 38$, $b_\phi = 7$ and $b_\psi = 9$ this number is 18.921 (719 bits in total). Assuming a feedback rate of two bits/symbol/subcarrier, 10 OFDM symbols are needed to convey this information. This corresponds to a time of 0.076ms per mobile-station (assuming the feedback is performed in a TDMA manner) including a 40μs preamble. The IEEE802.11ac standard defines a procedure where several frames are being exchanged during the feedback procedure. This procedure is outlined in Section II of [17]. The signalling includes null data packet announcement, null data packet, beamforming report poll and short inter-frame spacing which amounts to an additional 0.366ms. In total the overhead would thus becomes 0.564ms. Assuming an update cycle of 23ms, the feedback overhead is only 2.5%. With an update rate of 3ms, the overhead becomes 18.8%. The reason for the large additional overheads (null data packet announcement, null data packet, beamforming report and short inter frame spacing) is the compatibility with the contention based channel access (CS/CSMA) of 802.11 standards. If the timeslots of these transmissions could be pre-reserved, and the header reduced from 40μs to 3 OFDM symbols, the overheads would reduce to only 0.7% and 5.4%, for an update rate of 23ms and 3ms, respectively (this would also require that the pilot symbols of the null data packet where piggy backed on the last transmission from the BSs).

The paper [17] also investigates further reductions in the overhead by utilizing the correlation between adjacent channel estimates, which would be applicable to our scenario as well.

C. Beamformers

In the IA case, the beamformers are first initialized in the closed form solution given in Appendix II of [3]. This solution is then refined using twelve iterations of the max-SINR method given in [19]. This method aims to optimize the SINR of each of the three users. This SINR can be expressed as

$$\text{SINR}_k = \frac{|\mathbf{u_k}^H \mathbf{H}_{k,k} \mathbf{v}_k|^2}{\sum_{j=1}^{K} |\mathbf{u_k}^H \mathbf{H}_{k,j} \mathbf{v}_j|^2 + \sigma^2}, \quad (3)$$

using the notations of [19]. We employ the iterative max-SINR algorithm also in the CoMP case. In this case the channel matrices in (3) are of size 2×6, and only one channel matrix is used per MS. We initialize the transmit beamformers in the pseudo-inverse of the eigenbeamformers for the three users.

The beamformers are calculated for the subcarriers where the channel is fed back, see Section III-B, and re-used on adjacent subcarriers.

IV. RF Impairment Model

Since we perform measurements of real-world transmission over a wireless channel, we do not need a propagation model, nor do we need a hardware impairment model. However, the use of RF-impairment models is becoming a popular way of bringing realism to simulations and analysis of wireless systems. We therefore include results, where we use simulations on the estimated channels from the measurements, and compare with the actual transmission results from the same measurements. This is done in order to investigate the accuracy of this type of modeling. In addition, we also use this modeling to extrapolate our results to a shorter feedback update interval than we have actually implemented, More on this will follow in Section V-C.

The impairment model used for the transmitter is illustrated by Figure 4 and is similar to the simplified model in Section 7.2.2 of [7] with negligible IQ imbalance (the parameters $\mathbf{K}_1$ and $\mathbf{K}_2$ of [7] become an identity- and zero-matrix, respectively).

Some recent work has also used a similar model for finding globally optimal beamformers for multicell MISO networks [20], and for finding locally optimal precoders for multi-cell MIMO networks [21]. However, the model is applied subcarrier-by-subcarrier in [20] and [21], for mathematical tractability.

The impaired signal is obtained from the ideal by multiplying all subcarriers with a common phasor $\exp(j\theta(t))$. This phase rotation is known as the common phase error (CPE); see e.g. [7], since it affects all subcarriers in the same way. However, since each of the six transmitters in our system employs its own PLL-based local oscillator (LO), it can be regarded as independent between transmitters - which deteriorates beamforming performance.

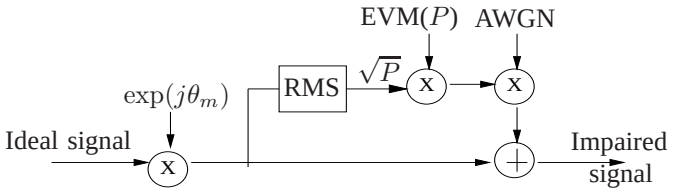

Fig. 4. Impairment model for the transmitter

As shown in Figure 4 an additive white Gaussian noise (AWGN) (complex circular symmetric) is added to the received signal. The power of this noise is governed by the root-mean-square (RMS) of the input signal and the error-vector-magnitude (EVM) parameter. The EVM is in general a function of the power of the signal and is a measure of the modulation accuracy achieved by the transmitter. The use of a AWGN source is motivated in e.g. [22], and has been used also in [23]. In the receiver we use the same impairment model as in the transmitter, but without any CPE. Since our receivers use a common LO in its two receiver branches, the impact of the CPE should be negligible. In the sequel, we will sometimes refer to our impairment model as "the EVM model".

In Figure 5 below we have plotted the EVM of our six transmitters as a function of the output power. The EVM was measured by capturing the output using a spectrum analyzer. The signal transmitted was a plain OFDM signal with 16QAM constellation generated according to our parameters. The received signal was processed in Matlab where channel estimation was performed first, followed by CPE correction based on the pilot subcarriers. The EVM is then calculated based on the received constellation points (see also http://en.wikipedia.org/wiki/Error_vector_magnitude). The rise at high power levels is due to the compression in the power amplifiers. The output power was rarely above 13dBm from any single amplifier during the measurements presented in Section V. The standard deviation of the CPE varies from 0.62 degrees to 1.5 degrees. The distribution of the CPE can be characterized as Laplacian.

The EVM of our receivers is shown in Figure 6. These measurements were performed using a high quality signal generator as input source. The rise at low input levels is due to the impact of thermal noise. The curves shown in Figure 5 and 6; are first used as look-up tables when performing simulations using the impairment model. More details of the use of the model is provided in Section V-C.

V. Results

A. Raw results

The measurements were performed as follows. The three MSs were placed in random locations. The IA scheme is then run first followed by CoMP 0.34 seconds later. After this three reference schemes are run one at a time. The three reference schemes are "TDMA MIMO", "full-reuse SIMO" (FR SIMO) and "full-reuse MIMO" (FR-MIMO). In TDMA MIMO, only one BS-MS pair is active at a time. But instead

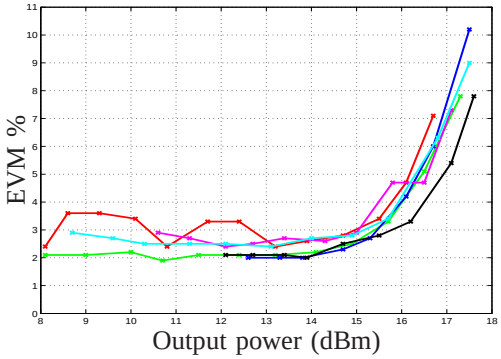

Fig. 5. EVM measurements on the transmitters

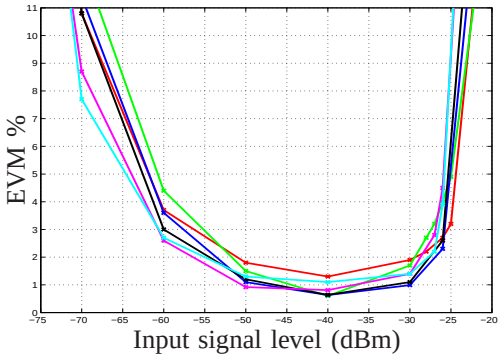

Fig. 6. EVM measurements on the receivers

two streams are active simultaneously. In FR-SIMO each base-station transmits simultaneously using one antenna. In FR-MIMO, all links are active at the same time using two streams each i.e. six streams are active in total. None of the reference schemes use beamforming in the transmitter and therefore no feedback according to Section III-B is needed in these schemes. All the schemes are run three times in every location. For every location we also perform measurements with one person walking in the measurement area and with two persons walking in the measurement area. This gives us the possibility to analyze the influence of channel variations in a typical office scenario with increasing mobility. The three MSs are then moved to new random location and the entire sequence is repeated.

In total 21 locations were tried. The first 10 were in line-of-sight (LoS), which means that all three MSs were in the corridor, see Figure 1, while the last 11 where in NLoS i.e. the three MSs were located in the rooms adjacent to the corridor.

The performance in LoS and NLoS scenarios is illustrated by the solid lines in Figure 7 and 8. The gain of IA and CoMP over the best reference scheme is summarized in Table I (the red italic numbers will be explained in Section V-C). The reason for better IA results in NLoS is the better isolation of the cells in terms of path-loss, as was shown in [12]. We note that IA deteriorates with increasing mobility, while it still able to provided a gain over the reference schemes. The fact that IA is always better than FR-SIMO also proves that the transmitter beamforming is effective. CoMP is more robust

LoS		
	IA	CoMP
Stationary	14%	33%
One person walking	10%	32%
Two persons walking	3.5% *10%*	36%
NLoS		
	IA	CoMP
Stationary	37%	59%
One person walking	32%	61%
Two persons walking	26% *33%*	50%
LoS+NLoS		
	IA	CoMP
Stationary	27%	47%
One person walking	23% *24%*	49%
Two persons walking	16% *24%*	45%

TABLE I
GAIN OF IA AND COMP OVER BEST REFERENCE WITH 23MS UPDATE RATE AND 2.5% OVERHEAD DEDUCTED. RED ITALIC NUMBERS ARE PREDICTIONS OF THE PERFORMANCE WITH 3MS UPDATE RATE AND 5.4% OVERHEAD, SEE SECTION V-C

to the channel variations than IA. The reason could be that CoMP will utilize strong channel elements more than IA. The relative change of weak channel elements is typically much faster than strong channels (e.g. a channel in a deep fade).

B. Results with ideal hardware

In order to investigate the "would-be" performance with perfect hardware, simulations are performed where the transmitted signals are convolved with the measured channels. The exact same code (software) is used for the transmitter and receiver processing as in the real-time evaluations. The channels are estimated from the C0-C5 pilots in the frames (see above). The same pilot symbols are used throughout the air interface (orthogonality is achieved through time multiplexing). This implies that non-linearity effects should always appear identically at the transmitter each time the pilot is transmitted. If this is not the case, the channel estimates will vary between frames even if the true channel does not - and this will be erronously appear as channel variations.

The result for the LoS and NLoS case is shown by the dashed lines in Figure 7 and 8, respectively. The LoS results show that sum throughput of IA increases 30-40% with perfect hardware, while CoMP and TDMA MIMO improves 25-30%. The performance of FR-SIMO and FR-MIMO changes insignificantly. In the NLoS scenario, the performance improvement is 20% for IA, 10% for CoMP and 30-40% MIMO. We note that IA and MIMO rely on suppression of interference using a minimal number of antennas, and this may be the reason for their larger vulnerability to hardware impairments as well as channel variations.

C. Impairment model analysis

In Section IV we introduced an impairment model. In previous section we simulated the performance of ideal hardware by convolving the transmitted signal with the exact channels measured during the "real-time" measurements presented in Section V-A. Here we modify this procedure by processing

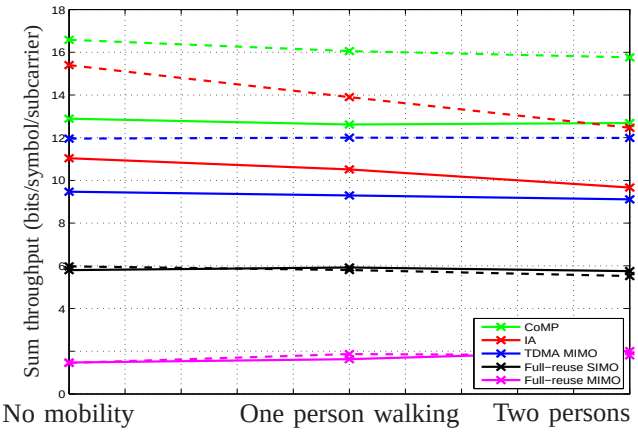

Fig. 7. Sum throughput LoS measurements. The dotted lines shows the "would-be" performance with perfect hardware.

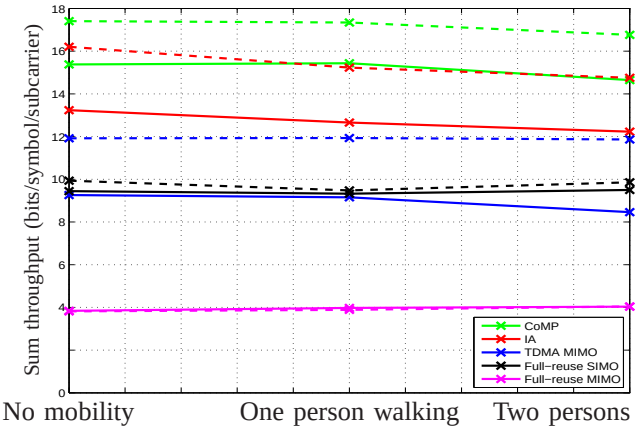

Fig. 8. Sum throughput NLoS measurements. The dotted lines shows the "would-be" performance with perfect hardware.

the transmit signals using the impairment model of Section IV before convolving with the measured channels. In addition we also feed the received signal through the impairment model at the receiver. The CPE is modeled as Laplacian with 1.5degrees standard deviation based on our worst case measurement. The RMS value of the signals are calculated per OFDM symbol. The EVMs are based look-up tables for each transmitter and receiver based on the measurements shown in Figure 5 and Figure 6. The result (Los and NLoS combined) is shown in Figure 9. The EVM model still over-estimates the performance by 9-21% in the IA and CoMP cases, and 6-14% in the TDMA-MIMO case.

Using the EVM-model we are able to estimate the performance using 3ms update rate. We do this by selecting the channel estimates from the first subframe for the beamformer calculation (rather than the channel estimates from the training frame) [1]. We then evaluate the performance on all six subframes using the channels of those subframes. The results are summarized in Table II, for different update rates (disregarding

[1]Note that the update rate is not directly a parameter of the EVM-model but a consequence of the channel estimates we use for emulating the propagation channel

Scheme	23ms actual stationary	23ms EVM-model stationary	3ms EVM-model two persons walking
LoS			
IA	11.0	13.0	12.8
CoMP	12.9	15.3	15.8
TDMA-MIMO	9.5	10.3	10.3
FR-SIMO	5.8	5.7	5.3
FR-MIMO	1.5	1.4	1.8
NLoS			
IA	13.2	15.0	15.1
CoMP	15.4	17.2	17.3
TDMA-MIMO	9.3	9.9	9.7
FR-SIMO	9.4	9.6	9.4
FR-MIMO	3.8	3.8	4.0
LoS+NLoS			
IA	12.2	14.0	14.0
CoMP	14.2	16.3	16.6
TDMA-MIMO	9.4	10.1	10.0
FR-SIMO	7.7	7.7	7.4
FR-MIMO	2.7	2.6	3.0

TABLE II
SUM THROUGHPUT IN BITS/SYMBOL/SUBCARRIER USING THE REAL-SYSTEM AND EVM-MODEL - DISREGARDING FEEDBACK OVERHEAD

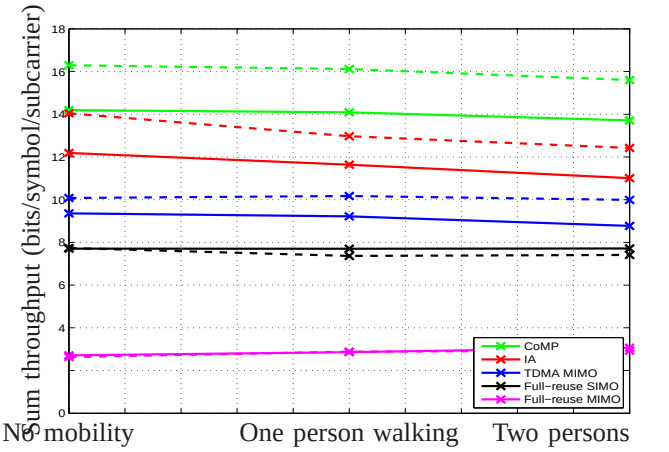

Fig. 9. Sum throughput LoS+NLoS measurements. The dotted lines shows the results of the EVM-model.

overheads). The results show that with the 3ms update, the performance can be brought back to that of the stationary channel using the EVM model.

Based on this result, we assume that the performance of the real system will also return to that of the stationary case, with the 3ms update rate. In Section III-B we calculated the feedback overhead according to the IEEE802.11ac standard to be 2.5% and 18.8%, at 23ms and 3ms update intervals, respectively. The additional overhead of going to a 3ms update interval does not pay off. However, assuming that some of the overhead signaling of IEEE802.11ac could be avoided would bring the overhead down to 5.4%. Under this assumption the performance of IA improves with the 3ms update rate while CoMP improves only marginally in a few cases. The gain of IA with this reconfiguration is 10-33% as shown in red in italic Table I.

VI. CONCLUSION

We have implemented IA and CoMP on a system consisting of three BSs and three MSs each having two antennas. The sum throughput of the system has been studied and compared with reference schemes such as TDMA MIMO and FR SIMO. Theoretically, at high SNR the gain of IA over TDMA should be 50% based on a degrees of freedom analysis. The closest we get to this number is in the NLoS stationary scenario where the gain is 27%. However, this gain drops when there are people walking in the environment. *However, there is still a gain even for the time varying channel and with the overheads.*

In the LoS scenario, gains with IA are small. This is due to the worse path-loss ratios (cell isolation) in this scenario as we showed already in [12].

Coordinated multipoint (CoMP) provides a gain over the reference schemes in both LoS and NLoS, 33% and 59%, respectively, and seems to be robust to channel variation induced by walking people.

Our results showed that our hardware reduces the performance by some 10%-40%. It should be kept in mind that the EVMs measured on our equipment are in the range of what could be expected on consumer-grade equipment. An impairment model based on EVM measurements of our testbed hardware was used and compared with the actual results. The model does bring us closer to the real system but there is still an overestimation of the performance. This shows the necessity of incorporating the impact of RF impairments in the analysis of advanced MIMO techniques and the importance of experimental performance evaluations.

REFERENCES

[1] D. Gesbert, S. Hanly, H. Huang, S. S. Shitz, O. Simeone, and W. Yu, "Multi-cell MIMO cooperative networks: A new look at interference," *IEEE Journal on Selected Areas in Communication*, vol. 28, no. 9, pp. 1380–1408, 2010.

[2] D. Lee, S. Hanbyul, B. Clerckx, E. Hardouin, D. Mazzarese, S. Nagata, and K. Sayana, "Coordinated multipoint transmission and reception in lte-advanced: deployment scenarios and operational challenges," *IEEE Communications Magazine*, vol. 50, no. 2, pp. 148–155, 2012.

[3] V. Cadambe and S. Jafar, "Interference alignment and degrees of freedom of the K -user interference channel," *IEEE Transactions on Information Theory*, vol. 54, no. 8, pp. 3425 –3441, aug. 2008.

[4] R. Brandt, P. Zetterberg, and M. Bengtsson, "Interference alignment over a combination of space and frequency," in *Proceedings IEEE International Conference on Communications*, 2013.

[5] C. Yetis, G. Tiangao, S. Jafar, and A. Kayran, "On feasibility of interference alignment in mimo interference networks," *Signal Processing, IEEE Transactions on*, vol. 58, no. 9, pp. 4771–4782, 2010.

[6] R. Tresch and M. Guillaud, "Clustered interference alignment in large cellular networks," in *IEEE International Symposium on Personal, Indoor and Mobile Radio Communications*, 2009, pp. 1024–1028.

[7] T. Schenk, *RF Imperfections in High-Rate Wireless Systems: Impact and Digital Compensation*. Springer, 2008.

[8] O. E. Ayach, S. Peters, and R. Heath, "The feasibility of interference alignment over measured MIMO-OFDM channels," *IEEE Transactions on Vehicular Technology*, vol. 59, no. 9, pp. 4309 –4321, nov. 2010.

[9] Ó. González, D. Ramírez, I. Santamaria, J. García-Naya, and L. Castedo, "Experimental validation of interference alignment techniques using a multiuser MIMO testbed," in *Smart Antennas (WSA), 2011 International ITG Workshop on*, feb. 2011.

[10] J. García-Naya, L. Castedo, Ó. González, D. Ramírez, and I. Santamaria, "Experimental evaluation of interference alignment under imperfect channel state information," in *European Signal Processing Conference (EUSIPCO 2011)*, Barcelona, Spain, aug. 2011.

[11] P. Zetterberg and N. Moghadam, "An experimental investigation of SIMO, MIMO, interference-alignment (IA) and coordinated multi-point (CoMP)," in *International Conference on Systems, Signals and Image Processing (IWSSIP)*, April 2012.

[12] P. Zetterberg, "Interference alignment (IA) and coordinated multi-point (CoMP) with IEEE802.11ac feedback compression: testbed results," in *Submitted to ICASSP 2014*, 2014, http://arxiv.org/abs/1311.1013.

[13] V. Jungnickel, A. Forck, S. Jaeckel, F. B. S. W. S, L. Thiele, . T. Haustein, W. Kreher, J. Mueller, H. Droste, and G. Kadel, "Field trials using coordinated multi-point transmission in the downlink," in *3rd International Workshop on Wireless Distributed Networks (WDN), held in conjunction with IEEE PIMRC 2010*. IEEE, September 2010.

[14] D. Li, Y. Liu, H. Chen, Y. Wan, Y. Wang, C. Gong, and L. Cai, "Field trials of downlink multi-cell MIMO," in *Wireless Communications and Networking Conference (WCNC), 2011 IEEE*, march 2011, pp. 1438 –1442.

[15] J. Holfeld, I. Riedel, and G. Fettweis, "A CoMP downlink transmission system verified by cellular field trials," in *European Signal Processing Conference (EUSIPCO)*, aug. 2011.

[16] P. Zetterberg, "Wireless development laboratory (WIDELAB) equipment base," S3, Royal Institute of Technology, Tech. Rep. (IR-S3-SB-0316), March 2003, available at http://www.ee.kth.se/ perz/cv/widelab.pdf.

[17] R. Porat, E. Ojard, N. Jindal, M. Fischer, and V. Erceg, "Improved MU-MIMO performance for future 802.11 systems using differential feedback," in *UCSD Information Theory and Applications Workshop*, Catamaran Resort, San Diego, USA, 2013, pp. 1–5.

[18] J. Roh and B. Rao, "Efficient feedback methods for MIMO channels based on parameterization," *IEEE Transactions on Wireless Communications*, vol. 6, no. 1, pp. 282–292, 2007.

[19] K. Gomadam, V. Cadambe, and S. Jafar, "Approaching the capacity of wireless networks through distributed interference alignment," in *IEEE Global Telecommunications Conference, 2008 (GLOBECOM 2008)*, 30 2008-dec. 4 2008, pp. 1 –6.

[20] E. Björnson, P. Zetterberg, and M. Bengtsson, "Optimal coordinated beamforming in the multicell downlink with transceiver impairments," in *Global Communications Conference (GLOBECOM), 2012 IEEE*, 2012, pp. 4775–4780.

[21] R. Brandt, E. Björnson, and M. Bengtsson, "Weighted sum rate optimization for multicell MIMO systems with hardware-impaired transceivers," in *IEEE Conf. Acoust., Speech, and Signal Process. (ICASSP'14)*, 2014.

[22] E. Costa and S. Pupolin, "M-QAM-OFDM system performance in the presence of a nonlinear amplifier and phase noise," *IEEE Transactions on Communications*, vol. 50, no. 3, pp. 462 –472, mar 2002.

[23] B. Göransson, S. Grant, E. Larsson, and Z. Feng, "Effect of transmitter and receiver impairments on the performance of MIMO in HSDPA," in *IEEE 9th Workshop on Signal Processing Advanced in Wireless Communications*, 2008, pp. 496–500.